

Measurement of deuteron spectra in Low Earth Orbit with the Alpha Magnetic Spectrometer

G. Lamanna, B. Alpat, R. Battiston, B. Bertucci, W. J. Burger, G. Esposito, E. Fiandrini, and P. Zuccon

University and INFN Perugia

Abstract. A high statistics measurement of the deuteron spectrum over the kinetic energy per nucleon range 90 to 850 MeV/n , at several magnetic latitudes, was performed by the Alpha Magnetic Spectrometer (AMS) during the Shuttle flight STS-91 at altitudes near 380 km on a 51.7° orbit. Above the geomagnetic cutoff the observed deuteron flux is compatible with Leaky Box Model predictions. Below the geomagnetic cutoff a second spectrum was observed.

flew a precursor mission in June 1998 on board the space Shuttle Discovery during flight STS-91 at altitudes between 320 and 390 km. In this report we use the data collected during the flight to study the D spectra in the kinetic energy range 90 to 850 MeV/n . The high statistics allows the measurement of the spectrum at several geomagnetic latitudes.

1 Introduction

The rare hydrogen isotopes in cosmic rays are generally believed to be of secondary origin, resulting mainly from the nuclear interactions of primary cosmic-ray protons and ^4He with the interstellar medium. It is expected that they provide important information concerning the propagation of cosmic rays in the interstellar space (Stephens (1989)) (Seo et al. 1 (1994)). Most previous D abundance measurements have been at energies $\leq 100 MeV/n$ (Seo et al. 1 (1994)), where the solar modulation effects are large and the presence of an anomalous He component complicates the interpretation of the data. The identification of deuteron nuclei, specifically at energies greater than 100 MeV/n is difficult due to the high experimental mass resolution required to distinguish those nuclei from the abundant background of protons. There are few deuteron measurements at these energies from balloon-borne experiments. For these measurements, however, the correction for $\sim 5 g/cm^2$ of residual atmosphere is an important source of systematic error. The flux of atmospheric secondary deuterons, with energy $\leq 600 MeV/n$, at typical balloon altitudes, is of the order of the measured fluxes (Lamanna 2 (2000)).

The Alpha Magnetic Spectrometer (AMS) is a high energy physics experiment scheduled for installation on the International Space Station. In preparation for this mission, AMS

2 The AMS experiment

The major elements of AMS as flown on STS-91 mission were a permanent magnet with an analyzing power, $BL^2 = 0.14 Tm^2$, a six layer silicon tracker, Time-of-Flight (ToF) hodoscopes, a Čerenkov counter and anti-coincidence scintillator counters. More details of AMS detector can be found in (Alcaraz 1 (2000)). In flight the AMS positive z-axis was pointing out of the Shuttle payload bay which was oriented at different angles with respect to the zenith: 0° , 20° and 45° , for 19, 25 and 20 hours respectively. Data from these directions are referred to as “downward” going. During the last 11 hours of the mission, AMS was pointing towards the Earth. Events from this last period are referred to as “upward” going.

3 Analysis

Deuteron candidates were selected by requiring the measured particle charge to be $Z = 1$ and reconstructed mass compatible with the deuteron one.

The possible backgrounds arise from two different sources:

- 1) $Z = 2$ particles with wrongly measured charge. In order to remove this background the consistency of the charge measurements was required from both the time of flight and the tracker. This source of background was consequently reduced at a negligible level: $< 10^{-5}$.
- 2) Proton events with wrongly reconstructed velocity and/or momentum. This background was reduced by applying the following selection criteria: a) At least three matched hits in

Correspondence to: G. Lamanna // (Giovanni.Lamanna@cern.ch)

the four time of flight planes were required. Such a criteria reduced tails in the distribution of the time of flight and in the distribution of the difference between, the position of the hits on the ToF counters and the position extrapolated from tracker. b) Cuts on the χ^2 value of the fitted particle trajectory were applied to remove tracks with a single large scattering. c) Agreement between the rigidity measured with the first three hits along the track, with the last three hits and with all the hits, was required, removing events with track affected by any multiple large angle scattering.

The resulting average selection efficiency was $\sim 53\%$.

Due to the AMS momentum resolution a small irreducible background from proton events survived.

The exact evaluation of the background was done using the distribution of the inverse of the momentum, $\frac{1}{p}$ which is approximately Gaussian. Events were divided in several velocity intervals ($\beta_i, \beta_i + \Delta\beta$) with $\Delta\beta$ approximately comparable with the velocity resolution.

Such a selection is useful to divide events in approximately mono-energetic samples and achieve the identification of the irreducible proton background. Several $\frac{1}{p}$ histograms were analyzed from $\beta_{min}=0.4$ to $\beta_{max}=0.85$ which correspond to the momentum range for deuterons of $0.9 < p < 3.0 \text{ GeV}/c$. The proton and deuteron Monte Carlo (MC) simulations reproduced the $\frac{1}{p}$ histograms within 1-2 %. A Gaussian fit of the data and MC histograms was performed.

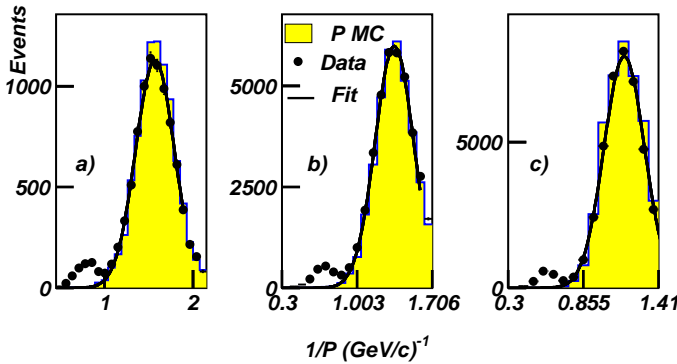


Fig. 1. Example of $1/p$ histograms for several β ranges: a) $0.55 < \beta \leq 0.575$; b) $0.575 < \beta \leq 0.65$; c) $0.65 < \beta \leq 0.7$. Protons Monte Carlo (yellow shadowed histogram) and protons Gaussian fit (line) overlapped to data (full circle markers). The deuteron candidates appear on the left side of the distribution.

The fitted proton background was then subtracted from the data in each $\frac{1}{p}$ distribution in order to select the most reliable samples of deuterons versus the momentum (Fig. 1). Figure 2 shows an example of final mass distribution for protons, resulted from the MC fit procedure and deuterons after the proton background subtraction.

The accepted deuterons are reconstructed in the range of mass from 1.55 to $2.7 \text{ GeV}/c^2$ where the tail of subtracted protons was about $10 \pm 2\%$ of all the events. After subtraction the residual background falls well below 1%.

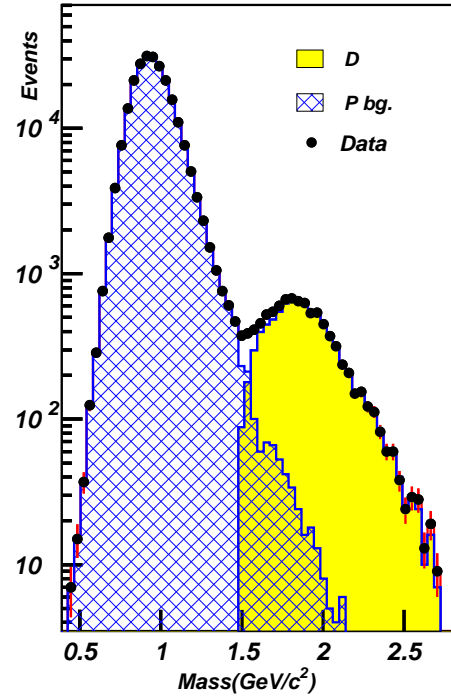


Fig. 2. Mass distribution for most of the cosmic ($\Theta_M > 1$) D events (shadowed histogram), after irreducible proton background subtraction and protons selected (crossed histogram) according to the procedure discussed in the text, for ($\beta < 0.85$ and $R < 3 \text{ GV}$). Full circle markers are for the total mass distribution from data.

4 Deuteron differential energy spectra

The differential D flux was determined by correcting the measured rates for the detector acceptance as a function of the momentum and the direction of the particles. The amount of material at normal incidence was $1.5 \text{ g}/\text{cm}^2$ in front of the TOF system and $3.5 \text{ g}/\text{cm}^2$ in front of the tracker. The response of the detector was simulated with the AMS detector simulation program which is based on the GEANT package (Brun et al. (1987)). The effects of energy loss, multiple scattering, interactions (Aamio et al. (1990)) (Sorge (1995)), decays and the measured detector efficiency and resolution were included.

The overall correction due to deuteron interactions was found to be $11 \pm 3.5\%$.

The average acceptance was determined to be $0.167 \text{ m}^2 \text{ sr}$ in the examined energy range. Corrections to the acceptance due to trigger and offline selection were studied with a sample of events collected with an unbiased trigger and by comparing data and Monte Carlo samples.

The incident differential deuteron flux was obtained from the measured spectrum by unfolding the effect of the detector resolution. The detector resolution function was obtained from the simulation and an unfolding procedure, based on Bayes' theorem (details can be found in Lamanna 2 (2000)), was used. The average systematic uncertainty due to the full applied corrections in this analysis is 6.7 %.

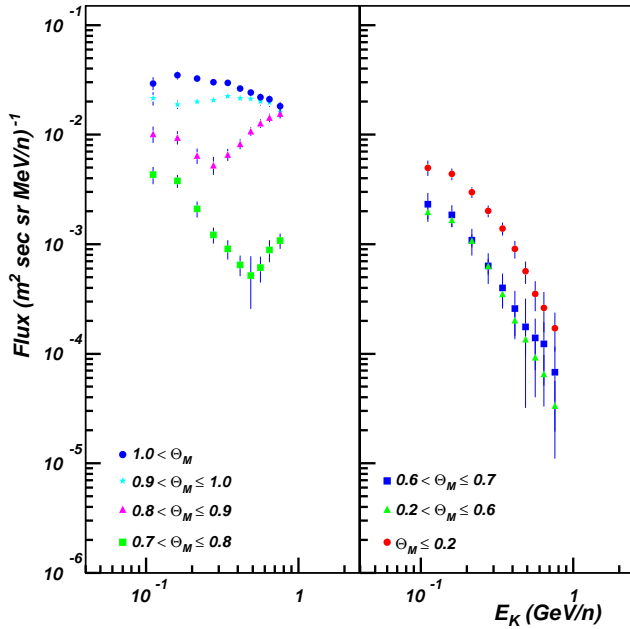


Fig. 3. Deuterons flux spectra separated according to the corrected geomagnetic latitude Θ_M . The error bars indicate the combined statistical and systematic uncertainties.

The differential energy deuteron spectra as a function of the incident kinetic energy per nucleon is shown in Fig. 3 for different geomagnetic latitude ($|\Theta_M|$) ranges. The figure shows the presence of cosmic spectrum for higher Θ_M , while for lower Θ_M latitudes, fluxes are affected by the geomagnetic cutoff, and finally it shows a second spectrum under cutoff at the lowest Θ_M .

4.1 Analysis of the cosmic spectrum

For the analysis of the cosmic deuteron spectrum the data above the geomagnetic cutoff from three AMS attitudes (0° , 20° and 45° with the zenith) have been considered. The deuterons fluxes measured with the all Shuttle orientations agree within the errors.

A total sample of $\sim 10^4$ deuterons were detected above the geomagnetic cutoff for $|\Theta_M| > 0.9$. Fig. 4 shows the final cosmic deuteron spectrum. A power-law spectrum in rigidity of the cosmic deuterons was then fitted to the solar modulation equation suggested in (Gleeson, Axford (1968)). The best fit of the data was obtained assuming a Local Interstellar Spectrum (LIS) with spectral index 2.75 and a modulation parameter $\phi=650 \pm 40$ MV.

The secondary-to-primary cosmic ray ratios are a significant way of testing the hypothesis of the nuclei propagation in the Galaxy. D is produced mainly from the spallation of ^4He and since D has the same charge-to-mass ratio as ^4He , it would be expected to be modulated like ^4He by the solar wind. The ^3He contribution to the total helium abundance is of the order of $\sim 10\%$, with an expected fluctuation of 1% due to the 11-year solar cycle. The deuteron-to-helium

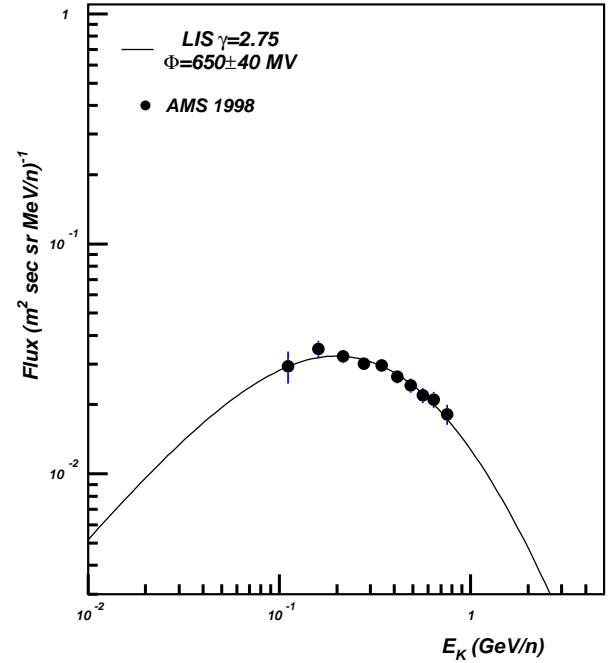


Fig. 4. Differential cosmic deuteron spectrum. The solid curve represents the best fit of data considering a LIS index 2.75 and resulting in solar modulation parameter $\phi=650 \pm 40$ MV.

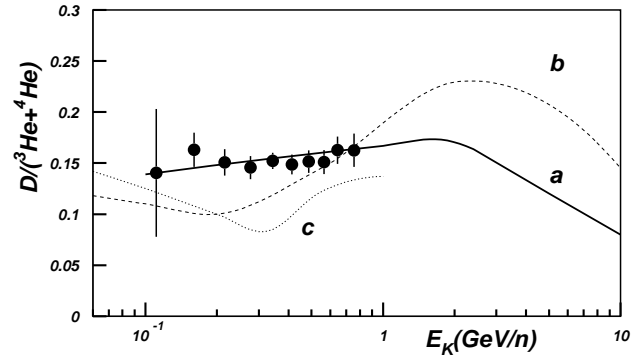


Fig. 5. Deuteron-to-helium ratio as measured from AMS compared with three different models calculation: a) (Stephens (1989)); b) (Mewaldt (1989)); c) (Seo et al. 1 (1994)) (Seo et al. 2 (1994)).

(Alcaraz 3 (2000)) ratio measured by AMS (Fig. 5) is a clear indication of agreement between deuteron measurements and calculation based on Leaky Box Model. In particular the data exclude some models (Seo et al. 1 (1994)) (Mewaldt (1989)) and agree with the Stephens (1989) calculations with the following assumptions: unmodulated D spectrum with an index 2.75 and a mean free path $\lambda_c(\text{gr}/\text{cm}^2): 8[5.5/R_{GV/c}]^\delta$ ($\delta = 0.6$ for $R > R_c = 5.5 \text{ GV}/c$ and $\delta = 0$ for $R < R_c = 5.5 \text{ GV}/c$).

The deuteron-to-proton ratio is not suited to test propagation models since D and P spectra can be differently affected by solar modulation. Nevertheless at higher energy such a ratio measured by AMS confirms the agreement with the Stephens LBM prediction and excludes non-standard models as from

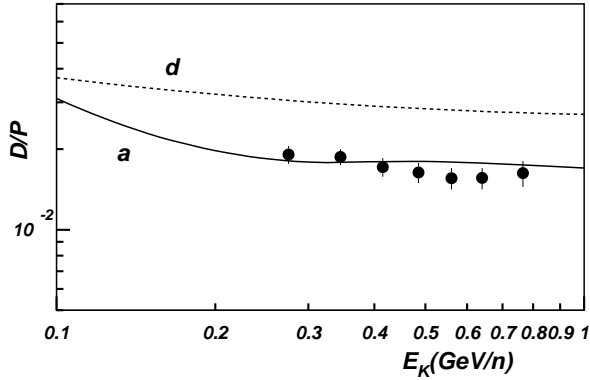


Fig. 6. Deuteron-to-proton ratio as measured from AMS compared with model predictions: a) Standard LBM prediction with Stephens assumptions (Stephens (1989)) (Seo et al. 1 (1994)); d) Stochastic reacceleration model prediction (Seo et al. 2 (1994)).

reacceleration theory (Seo et al. 2 (1994)).

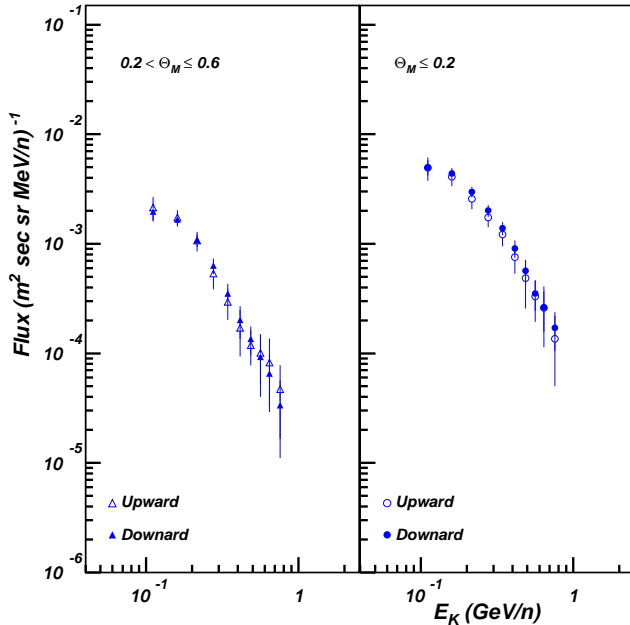


Fig. 7. Deuterons flux spectra separated according to the corrected geomagnetic latitude Θ_M . Below the geomagnetic cutoff, the upward and downward fluxes agree in the range $|\Theta_M| \leq 0.6$.

4.2 Analysis of the second spectrum

As shown in Fig. 7 a second spectrum of deuterons was detected below the geomagnetic cutoff. These spectra have the following properties:

- The second deuteron spectra are nearly constant over the wider interval $0.2 < |\Theta_M| \leq 0.6$ and show an enhancement of a factor 2 to 3 in the geomagnetic equator ($|\Theta_M| \leq 0.2$).
- At all latitudes the upward flux and the downward flux are comparable within the errors.

To understand the origin of the sub-cutoff spectrum, the

trajectories have been traced both backward and forward from their detection point using their incident angles and momenta, through the earth magnetic field, following the same procedure as described in (Alcaraz 1 (2000)) (Alcaraz 2 (2000)). The results of the tracing are the following:

- All deuterons were found to originate in the atmosphere.
- Analysis of the sum of their forward and backward flight times yields two distinct classes: “short-lived” (about 40%) and “long-lived” (60%) for flight times below and above 0.3 sec respectively.
- Most of the short-lived cross the equator only one time and the locations of their origin and destination are distributed uniformly around the globe.
- 90% of deuterons detected around the geomagnetic equator ($|\Theta_M| \leq 0.2$) resulted long-lived. They originate in the atmosphere in geographically restricted regions. They cross the equator tens of times and drift along the equator until the non-uniformities of the geomagnetic field return them to the atmosphere in distinct regions. The destination and origin regions matches those of the second long-lived protons and positrons detected by AMS (Alcaraz 1,2 (2000)).

e) The two classes are distinct also in terms of two classical parameters used to describe the particles trapping motion in the geomagnetic field: L -shell parameter and the equatorial pitch angle α_0 (Walt (1994)). The short-lived particles have spread L values distribution up to about $L=3$ and their α_0 distribution is peaked at low values (mostly $\alpha_0 < 50^\circ$). The long-lived particles are trapped in drift shell concentrated in the range $1 \leq L \leq 1.1$ and their α_0 are mostly around 80° , close to the maximum (90°) for the mirror points of each drift shell (Lamanna 1,2 (2000)).

Acknowledgements. I would like to thank the members of AMS collaboration and in particular Dr. V. Choutko for his help in performing this analysis.

This work has been partially supported by the Italian Space Agency (ASI) under contract ARS-98/47.

References

- Aamio P.A. et al., FLUKA Users Guide, CERN TIS-RP 190, 1990;
 Alcaraz J. 1, Phys. Lett. B 472, p. 215, 2000
 Alcaraz J. 2, Phys. Lett. B 484, p. 10, 2000
 Alcaraz J. 3, Phys. Lett. B 494, p. 193, 2000
 Brun R. et al., GEANT3, CERN-DD/EE/84-1 (Revised 1987).
 Gleeson L.J., Axford W.I. Astroph. Journal 154, p.1011, 1968
 Lamanna G. 1, Proc. Vulcano International Workshop, 2000
 Lamanna G. 2, PhD Thesis, Perugia, 2000; (available in <http://www.cern.ch/glamanna>)
 Mewaldt R.A., Proc. Cosm. Abund. of Matt., 183, p. 124, 1989
 Seo E.S. et al. 1, Astroph. Journal,432, p. 656, 1994
 Seo E.S. et al. 2, Astroph. Journal,431, p. 705, 1994
 Sorge H., Phys. Rev. C 52, p.3291, 1995.
 Stephens S.A., Adv. Space Res.,9, p. 145, 1989
 Walt M., Introduction to geomagnetically trapped radiation, Cambridge Press, 1994